Approximate analyses of reinforced concrete slabs

F.J. Vecchio† and M. Tata‡

Department of Civil Engineering, University of Toronto, Toronto, Ontario M5S 1A4, Canada

Abstract. Procedures are investigated by which nonlinear finite element shell analysis algorithms can be simplified to provide more cost effective approximate analyses of orthogonally-reinforced concrete flat plate structures. Two alternative effective stiffness formulations, and an unbalanced force formulation, are described. These are then implemented into a nonlinear shell analysis algorithm. Nonlinear geometry, three-dimensional layered stress analyses, and other general formulations are bypassed to reduce the computational burden. In application to standard patch test problems, these simplified approximate analysis procedures are shown to provide reasonable accuracy while significantly reducing the computational effort. Corroboration studies using various simple and complex test specimens provide an indication of the relative accuracy of the constitutive models utilized. The studies also point to the limitations of the approximate formulations, and identify situations where one should revert back to full nonlinear shell analyses.

Key words: analysis; deflection; finite elements; plates; reinforced concrete; slabs; stiffness; tests.

1. Introduction

Much progress has been made in recent years toward accurately modelling the behaviour of reinforced concrete shells through the development and application of nonlinear finite element procedures. Scordelis and Chan (1987) described a formulation based on a layered model applied to degenerate shell elements. Hinton and Owen (1984) produced a formulation of the same type. Various constitutive models and analysis procedures have also been presented by Hu and Schnobrich (1990), Polak and Vecchio (1993) and others. These formulations have generally been shown to provide reasonably accurate simulations of response under a variety of complex structural conditions and loading schemes.

While the aforementioned formulations vary widely in their approach to analysis methodology and constitutive modelling, they share the one characteristic inherent to all nonlinear shell formulations: they are computationally demanding. The complexity of the elements, typically coupled with a three-dimensional layered analysis, makes for numerically intensive and time-consuming calculations.

In many practical situations, the structures requiring analysis involve orthogonally reinforced flat plate elements subjected to transversely applied normal forces. In such cases, nonlinear

† Professor
‡ Graduate Student

geometric effects and in-plane load effects are largely insignificant. The modelling capabilities of a full nonlinear shell analysis are not required or effectively utilized. A simplified procedure, dispensing with some of the generality of a shell analysis while cutting down the computational effort, would be more cost effective with little loss in accuracy. In this regard, Scanlon (1971) described a successful implementation of Branson's effective stiffness formulations into a shell analysis algorithm. Jofriet and McNiece (1971) also reported some success in applying approximate methods in finite element analyses of reinforced concrete slabs. However, other attempts at developing simplified procedures specifically suited to the analysis of reinforced concrete flat plate structures are not well documented in the literature.

In this paper, alternative procedures for approximate deflection analysis of orthogonally reinforced plates are presented. Through sample analyses, and through comparisons with experimental data, the accuracy and limits of these procedures are discussed.

2. Finite element formulation

The analysis procedures discussed herein are predicated on modifications to a nonlinear finite element analysis program for reinforced concrete shells. The program used as a basis for this work was RASP, developed by Seracino (1995), which itself was a refinement of program APECS (Polak and Vecchio 1993).

Program RASP employs a nonlinear algorithm based on a full-load, secant-stiffness formulation. Concrete and reinforcement hysteretic behaviour, and other load-history effects, are enforced in the analysis algorithm through use of plastic offsets (Vecchio 1997). The material stiffness formulations are based on the smeared, rotating crack concept. Constitutive modelling is done according to the provisions of the Modified Compression Field Theory (see below).

Program RASP uses a heterosis-type degenerate isoparametric quadrilateral element (9-noded, 42 degree of freedom), based on Mindlin bending theory. A layered-element formulation is employed, providing a means to rigorously consider out-of-plane shear effects. Selective integration is used to avoid shear-locking and zero-energy problems. The resulting algorithm demonstrates good numerical stability and convergence. Further, it has been shown to provide accurate simulations of the response of reinforced concrete shell structures under a wide range of conditions. Further details on the finite element formulations and corroborations with experimental data are provided by Polak and Vecchio (1994).

Rigorous nonlinear analyses of shells are highly computation intensive and time consuming. If an effective simplified analysis procedure is to be used, it must be considerably simpler and quicker in its computational aspects. To this end, program SNAP was developed (Tata 1996). Based on RASP, it introduces the restrictions that the structure being analyzed be a flat plate, that the finite elements be rectangular, and that the reinforcement be orthogonal and aligned with the global coordinate system. This eliminates the need for several transformation calculations, thereby speeding up the analyses considerably. As well, the material is modelled as elastic, with effective stiffness parameters used to represent the variable stiffnesses arising from nonlinear effects. This eliminates the need for a layered element analysis in the main body of the finite element algorithm, thereby again considerably reducing the numerical demands of the process. The result is a much faster solution algorithm, requiring up to two orders of magnitude less computational time. Details of the modifications to the finite element modelling can be found in Tata (1996). Details of the models used to enforce the nonlinear behaviour in the simplified analyses are the

main concern of the discussions to follow.

3. Constitutive modelling

To accurately model the nonlinear behaviour of reinforced concrete, the use of realistic constitutive relationships is essential. Two of the three approximate analysis procedures to be presented will require such models. For these, the constitutive models of the Modified Compression Field Theory (MCFT) (Vecchio and Collins 1986) will be used. The constitutive models are summarized in Fig. 1; relevant formulations follow.

For normal strength concrete in compression, the Hognestad parabola is used as the base curve. The curve is modified to reflect compression softening effects, as follows:

$$f_{c2} = -f_p \left[2\left(\frac{\varepsilon_{c2}}{\varepsilon_p}\right) - \left(\frac{\varepsilon_{c2}}{\varepsilon_p}\right)^2 \right], \qquad 0 > \varepsilon_{c2} > \varepsilon_p \tag{1}$$

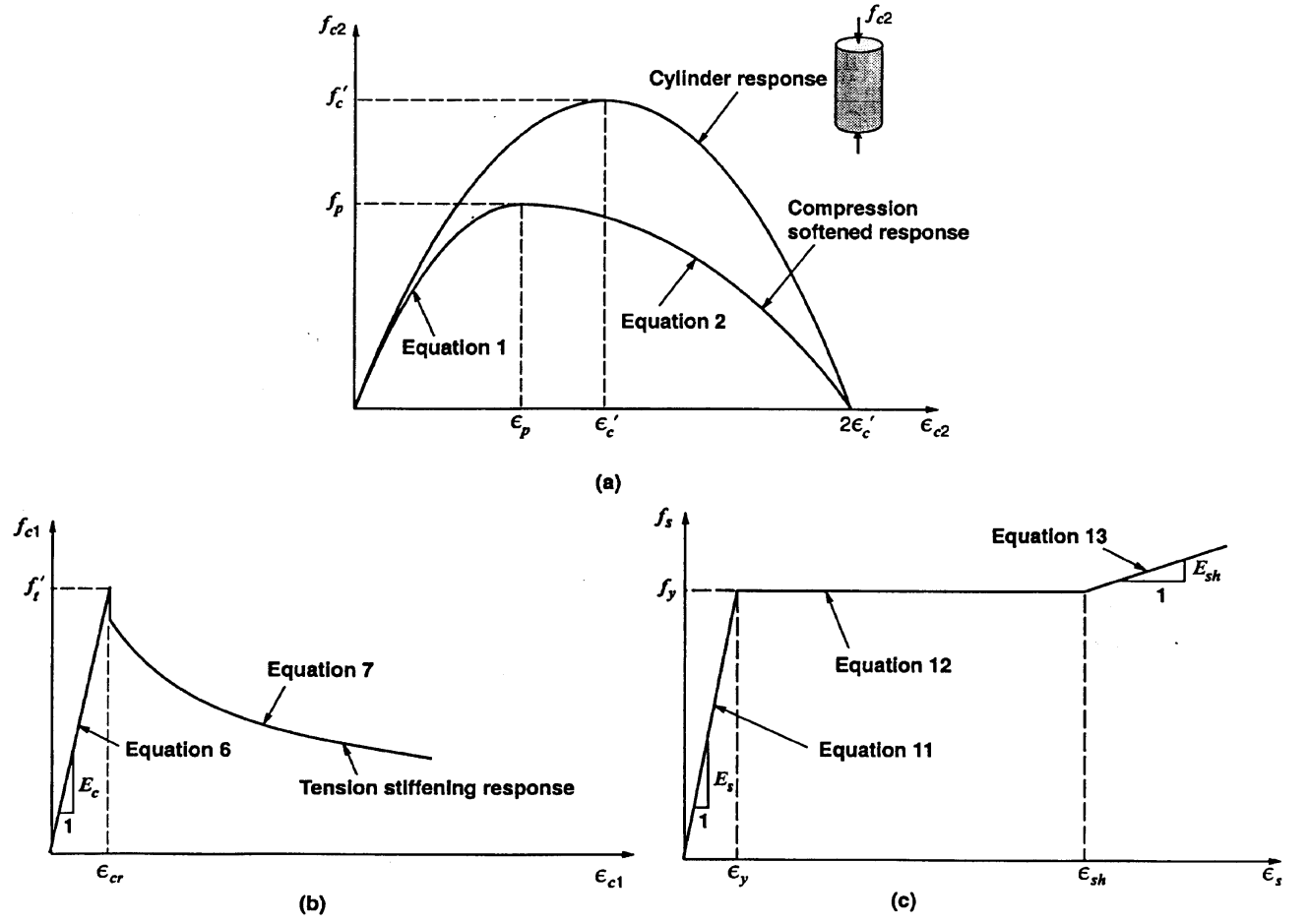

Fig. 1 Constitutive models: (a) Concrete in compression; (b) Concrete in tension; (c) Reinforcement in tension and compression

$$f_{c2} = -f_p \left[1 - \left(\frac{\varepsilon_{c2} - \varepsilon_p}{2\varepsilon'_c - \varepsilon_p} \right)^2 \right], \qquad \varepsilon_p > \varepsilon_{c2} > 2\varepsilon'_c \tag{2}$$

$$\varepsilon_p = \varepsilon'_c / \beta \tag{3}$$

$$f_p = f'_c / \beta \tag{4}$$

$$\beta = 0.8 - 0.27\left(\frac{\varepsilon_{c1}}{\varepsilon_{c2}}\right), \qquad \beta \geq 1 \tag{5}$$

where f_{c2} is the principal compressive stress, β is a reduction factor that takes into account compression softening due to the influence of tensile strains, f'_c is the concrete compressive cylinder strength, ε_c' is the concrete cylinder strain at peak compressive strength (negative quantity), ε_{c2} is the principal compressive strain (negative quantity), and ε_{c1} is the coexisting principal tensile strain (positive quantity). For high strength concrete, the Popovics formulation is substituted for the base curve. These formulations are discussed in detail by Vecchio and Collins (1993). If the concrete is in a state of biaxial compression, strength enhancement according to the Kupfer model is used.

For cracked concrete in tension, to correctly model effective stiffnesses at service load levels, it is essential to account for tension stiffening effects. This is done through use of the following relationships:

$$f_{c1} = E_c \cdot \varepsilon_{c1}, \qquad \varepsilon_{cr} > \varepsilon_{c1} > 0 \tag{6}$$

$$f_{c1} = \frac{f'_t}{1 + \sqrt{500\,\varepsilon_{c1}}}, \qquad \varepsilon_{c1} > \varepsilon_{cr} \tag{7}$$

$$E_c = \frac{-2f'_c}{\varepsilon'_c} \tag{8}$$

$$f'_t = 0.33\sqrt{f'_c} \quad \text{(MPa)} \tag{9}$$

$$\varepsilon_{cr} = \frac{f'_t}{E_c} \tag{10}$$

where f_{c1} is the principal tensile stress, f'_t is the tensile strength of the concrete, and E_c is the initial tangent stiffness. Coupled with this, however, one must check that the average tensile stresses can be transmitted across the cracks. This local crack check is done in the manner described elsewhere (Vecchio and Collins 1986).

The in-plane reinforcement, for both prestressed and nonprestressed types, is modeled by a simple trilinear function. The model is applied to reinforcement both in tension and compression; thus,

$$f_s = E_s \cdot \varepsilon_s, \qquad \varepsilon_s < \varepsilon_y \tag{11}$$

$$f_s = f_y, \qquad \varepsilon_y < \varepsilon_s < \varepsilon_{sh} \tag{12}$$

$$f_s = f_y + E_{sh} \cdot (\varepsilon_s - \varepsilon_{sh}), \qquad \varepsilon_s > \varepsilon_{sh} \tag{13}$$

where ε_s and f_s represent the strain and stress in the reinforcement, respectively; ε_y and f_y are the yield strain and yield stress, respectively; ε_{sh} is the strain at which work hardening begins; E_s is

the initial modulus of elasticity; and E_{sh} is the strain hardening modulus.

For the purposes of simplified analysis of plates, the material models presented above were implemented into a cross-sectional moment-curvature analysis algorithm (henceforth referred to as MOCA). A similar subroutine was previously successfully applied to the analysis of reinforced concrete frame (Vecchio and Emara 1992); further details can be found therein. Note that MOCA allows for the nonlinear analysis of a cross section, accounting for out-of-plane shear effects, by using a layered section approach. Each layer is considered to be under two-dimensional stress conditions, and each layer is analysed according to the compatibility and equilibrium conditions of the MCFT. In considering out-of-plane shear, a uniform shear strain distribution through the cross section is assumed. The merits and disadvantages of this assumption, as applied to beam sections, was discussed by Vecchio and Collins (1988).

4. Approximate analysis - Mode 1:

For transversely loaded plates at low and intermediate load levels, approximate analyses can be undertaken by utilizing Branson's formulation (1963) for effective stiffness. Although initially developed for deflection analysis of beams, Scanlon (1971) and others have shown that this empirical-based formulation provides reasonably good estimates of deflections of slabs at service load levels. However, it's application should be limited to cases where there is no yielding of the reinforcement at any location in the structure, and where there are no significant in-plane or torsional load effects.

Branson's formula for the effective moment of inertia of a cross section, I_{eff}, is:

$$I_{eff} = \left(\frac{M_{cr}}{M}\right)^3 \cdot I_g + \left[1 - \left(\frac{M_{cr}}{M}\right)^2\right] \cdot I_{cr} \tag{14}$$

$$M_{cr} = \frac{f_r I_g}{y_t} \tag{15}$$

$$f_r = 0.6\sqrt{f'_c} \quad \text{(MPa)} \tag{16}$$

where I_g is the gross moment of inertia, I_{cr} is the cracked moment of inertia, M is the bending moment acting on the section, M_{cr} is the cracking moment, f_r is the modulus of rupture, and y_t is the distance from the centroid to the tension face.

The above can be utilized in an iterative solution scheme. For each element, at each Gauss point, an estimate of the matrix of elastic rigidity [D] is required. Given the rigidity, an elastic analysis will yield the sectional forces M_x, M_y, and M_{xy}, calculated on a per unit width basis at each Gauss point. The influence of the torsional moments is obstensibly accounted for by adding or subtracting them from the normal moments, as appropriate, to produce the largest moment of the correct sense, thus:

$$M'_x = M_x + M_{xy}\,; \qquad M'_y = M_y + M_{xy} \tag{17}$$

These resultant moments are then inserted into Branson's formula to determine effective stiffness factors in the global x- and y-directions. Corresponding stiffness reduction factors, α_x and α_y, are calculated as follows:

$$\alpha_x = (I_{eff})_x / I_g\,; \qquad \alpha_y = (I_{eff})_y / I_g \tag{18}$$

The material constants are then multiplied by the stiffness reduction factors. In cracked concrete, Poisson's ratio is taken to equal zero. Thus,

$$E_x = \alpha_x E_c \; ; \qquad E_y = \alpha_y E_c \tag{19}$$

$$\nu_x = 0 ; \qquad \nu_y = 0 \tag{20}$$

$$G_1 = \alpha_x \alpha_y G ; \qquad G_2 = \alpha_x G \; ; \qquad G_3 = \alpha_y G \tag{21}$$

where

$$G = E_c / 2(1+\nu) = E_c / 2 \tag{22}$$

The revised stiffness matrix can then be recalculated as:

$$[D] = \begin{bmatrix} \frac{E_x \cdot t^3}{12} & 0 & 0 & 0 & 0 \\ 0 & \frac{E_y \cdot t^3}{12} & 0 & 0 & 0 \\ 0 & 0 & \frac{G_1 t^3}{12} & 0 & 0 \\ 0 & 0 & 0 & \frac{G_2 \cdot t}{1.2} & 0 \\ 0 & 0 & 0 & 0 & \frac{G_3 \cdot t}{1.2} \end{bmatrix} \tag{23}$$

where t is the thickness of the plate element.

As mentioned, $[D]$ is recalculated at each integration point of each element, and an elastic analysis of the structure is repeated. Iterations of the analysis are continued until satisfactory convergence of the stiffness reduction factors is achieved.

5. Approximate analysis - Mode 2:

The second approach to approximate analysis is similar to the first in that effective stiffness reductions factors are calculated and used. However, while the previous approach relied on an empirical formulation to supply the effective moment of inertia directly, the second mode utilizes appropriate constitutive relations contained within a layered cross sectional analysis algorithm. In doing so, it can more realistically model nonlinear behaviour at all stages of loading; most significantly, beyond the yielding and peak-capacity thresholds. As well, it can also explicitly take into account out-of-plane shear effects. However, the procedure is still restricted to considering transverse loads only, and makes no allowance for in-plane load effects.

The solution algorithm begins in much the same way as the first. From some estimate of the stiffness matrix $[D]$ at each integration point, an elastic plate analysis is done and the normal bending moments M_x and M_y, and the sectional shears V_x and V_y, are determined. As well, the analysis will give the strain conditions in the x- and y-directions at each integration point; these include the normal strains at mid-depth, ε_x and ε_y; the curvatures, ϕ_x and ϕ_y; the twist ϕ_{xy}; and the out-of-plane shear strains, γ_x and γ_y. To approximately account for torsional effects, the curvatures

are modified in analogous manner to the sectional moments in Mode 1; thus

$$\phi'_x = \phi_x + \phi_{xy}; \qquad \phi'_y = \phi_y + \phi_{xy} \tag{24}$$

For each of the two orthogonal directions, the strain measures (ε, γ, ϕ') are fed into MOCA, and corresponding sectional forces (N', V', M') are returned. The MOCA analysis is iterated, with the axial strain parameter ε adjusted until the net axial force on the section, N', converges to zero. The corresponding moment M' is then used to determine the stiffness reduction factor for that direction. Thus:

$$\alpha_x = \frac{M'_x/(\phi'_x \cdot E_c)}{I_g}; \quad \alpha_y = \frac{M'_y/(\phi'_y \cdot E_c)}{I_g} \tag{25}$$

The stiffness reduction factors α_x and α_y are then utilized in Eq. (23) to define an effective stiffness matrix [D] for the next iteration of calculations. The structure is reanalyzed until satisfactory convergence is achieved.

6. Approximate analysis - Mode 3:

In this third method of approximate analysis, nonlinearity is achieved without manipulation of the stiffness of the structure. Rather, nonlinear sectional analyses are conducted to identify unbalanced forces, and these are added to the global load matrix to satisfy compatibility conditions. The bending analysis is coupled with an in-plane finite element analysis to identify membrane force components. In this way, in-plane force effects are rigorously taken into account. Prestressing can thus also be considered.

Consider the case of axial force (F_a) acting on an element face; see Fig. 2. Beginning with the actual load on the structure, an initial linear elastic strain, ε_i, is estimated on the first iteration. This axial strain is fed into MOCA, which then returns an axial force (F_n) corresponding to the current strain level, according to the nonlinear constitutive models in effect. There will be a disparity between the force obtained from the finite element analysis (which assumed linear elastic uncracked behaviour), and that obtained from the nonlinear section analysis (MOCA). The difference between the two is termed the unbalanced force (F_u). The unbalanced force is added to a cumulative 'restoring force', F_r. The restoring force is added to the actual force, and the total force (F_t) is reapplied to the structure for the second iteration. It is evident that with further iterations, the accumulated restoring force will approach a value that yields a strain (ε_f) in the linear elastic structure equivalent to the strain produced by the actual force in the nonlinear element. In this manner, the nonlinear behaviour of the element is strictly enforced according to the governing constitutive relations.

In an analysis of a plate structure, separate bending and planar finite element analyses are performed using linear elastic uncracked section properties. These provide the element deformations. Average sectional axial strains, shear strains, and curvatures are determined for each element, in both the x- and y-directions, according to some preselected rule. For a particular element, one might use the average values from all nine integration points, or the values from the central node, or the maximums from any of the nine points. The corresponding restoring forces N_r, V_r, and M_r are calculated in the manner discussed above. The restoring moments on the section of the element in question are then calculated and applied as consistent nodal forces. Similarly, the

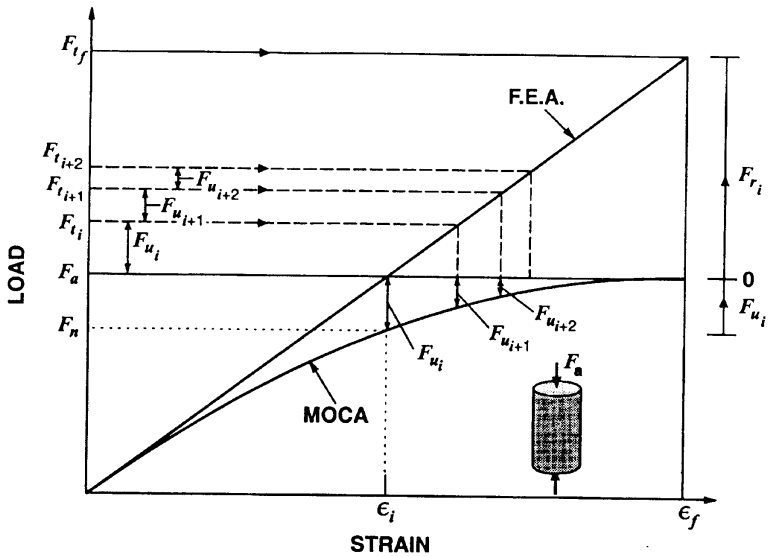

Fig. 2 Conceptual approach in Mode 3 approximate analysis (Unbalanced forces are defined and reapplied to structure)

restoring shears and axial forces are calculated and applied. The plate is reanalyzed, and the process is repeated until satisfactory convergence is achieved. Again, this results in nonlinear behaviour is strictly enforced. Full details of the formulation are described by Tata (1996).

Note that torsional moment effects are handled in the same manner as in Mode 1; that is, by adding the torsional moments to the normal moments produced by the linear elastic finite element analysis. These then add to the moments that must be balanced by the restoring forces, imposing additional straining on the structure.

7. Performance of analysis procedures

Through analyses of simple structures, an examination was made of the performance of the approximate analysis procedures. Program testing was based on an assessment of numerical accuracy, rate of convergence, and completion time. The numerical veracity of the element formulations were made using the patch test of Irons, as described by Cook (1989).

The patch tests were completed individually for constant moment and for constant stress in each of the orthogonal directions, for each of the approximate analysis procedures. The cross section used for the tests is that illustrated in Fig. 3(a), which had the moment-curvature response shown in Fig. 3(b) as computed using nonlinear sectional procedures. The structure modelled was a simple slab strip, 2000×1000 mm in dimensions, and represented by a grid of 4×2 finite elements. Shown in Fig. 3(c) are the element curvatures and internal moments evaluated at the central node of each element for the case where 0.80 M_u was applied as an end moment on the slab strips. Satisfactory numerical convergence and stability was achieved with all three analysis options. Note that the Mode 3 analysis, fully accounting for axial effects, typically required more iterations in order for the solutions to stabilize. Similar degrees of numerical accuracy were achieved in the other patch tests performated (Tata 1996).

Performance modelling was also scrutinized by conducting analyses of more representative structures, ranging from simple to more complex. One such analysis involved a cantilevered slab

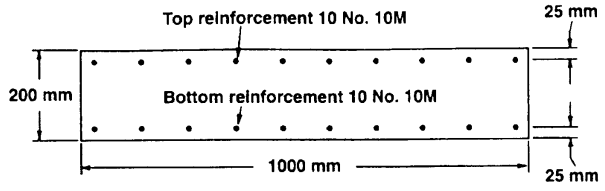

(a)

Concrete			Reinforcement					
f_c' (MPa)	ϵ_c' (mm/m)	f_t' (MPa)	A_s* (mm²/m)	E_s (MPa)	f_y (MPa)	f_u (MPa)	ϵ_{sh} (mm/m)	ϵ_u (mm/m)
30	-2.0	2.0	1000	200 000	400	600	10.0	50.0

* Per layer

	Element Number	X Direction			Y Direction		
		Mode 1	Mode 2	Mode 3	Mode 1	Mode 2	Mode 3
Curvature, ϕ ($\times 10^{-6}$/mm)	1	9.398	10.056	10.149	9.398	10.056	10.149
	2	9.398	10.056	10.149	9.398	10.056	10.149
	3	9.398	10.256	10.148	9.398	10.256	10.148
	4	9.398	10.255	10.148	9.398	10.255	10.148
	5	9.398	10.250	10.145	9.398	10.250	10.145
	6	9.398	10.250	10.145	9.398	10.250	10.145
	7	9.398	10.259	10.145	9.397	10.259	10.145
	8	9.398	10.259	10.145	9.398	10.259	10.145
MOMENT (kN·m/m)	1	54.6	54.7	54.5	54.6	54.7	54.5
	2	54.6	54.7	54.5	54.6	54.7	54.5
	3	54.6	54.7	54.5	54.6	54.7	54.5
	4	54.6	54.6	54.5	54.6	54.6	54.5
	5	54.6	54.6	54.5	54.6	54.6	54.5
	6	54.6	54.6	54.5	54.6	54.6	54.5
	7	54.6	54.6	54.5	54.6	54.6	54.5
	8	54.6	54.6	54.5	54.6	54.6	54.5
Number of Iterations		6	10	50	6	10	50

(c)

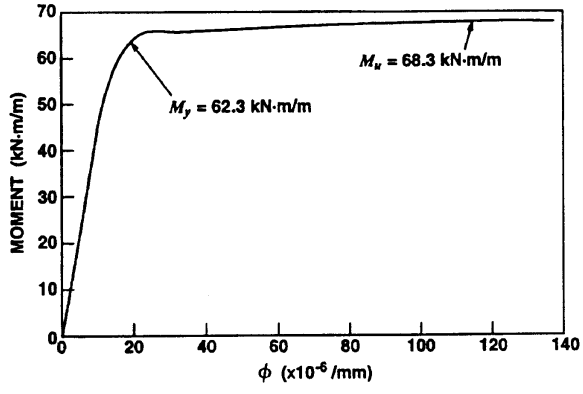

(b)

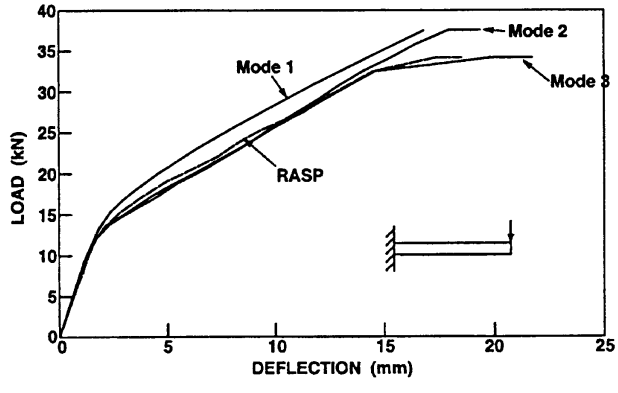

(d)

Fig. 3 Patch test for moment-curvature response: (a) Element cross section; (b) Theoretical response; (c) Predicted curvatures and moments; (d) Load-deflection response of a cantilevered slab

subjected to concentrated load along the free end. The slab section details were the same as those used for the patch tests, as were the slab dimensions. The slab was again modelled using a grid of elements consisting of 4 along the span and 2 across the width. The applied load was increased monotonically to failure. Shown in Fig. 3(d) are the resulting load-displacement responses as predicted by the three alternate approximate analyses and as predicted by a full nonlinear shell analysis (RASP). As can be seen, the three analyses provide surprisingly consistent results at low and intermediate load levels. Note too that the analysis results are very similar to those obtained from the RASP shell analysis. It should be remembered that in this case problem, shear, torsion, and axial load effects were insignificant.

With regards to numerical stability, each of the procedures was equally stable and compliant. However, typically the Mode 3 analyses required significantly more iterations to achieve convergence, whereas the Mode 1 analysis required the fewest. This had some impact on the relative job completion times. For example, consider the analyses associated with the patch test discussed above in which 0.80 M_u was applied to the slab strip. Using Mode 1 analysis, 5 iterations were required consuming a total of 9 seconds on a PC 486 processor. To achieve similar convergence, the Mode 2 and Mode 3 analyses required 12 iterations and 34 seconds, and

48 iterations and 130 seconds, respectively. A full shell analysis, on the other hand, required substantially more time.

8. Experimental corroboration

In addition to being numerically robust and reliable, the approximate analysis procedures must be examined for their ability to accurately simulate aspects of the nonlinear response of reinforced concrete slabs. Three series of concrete tests specimens were chosen for investigation. The first, owing to the simplicity of the test specimens, provided a more rigorous check of the basic constitutive modelling. The second series involved specimens significantly affected by two-way action, thus providing a check of the modelling of torsional moment effects. The last series examined, involving more complex specimens, provided a check of the influence of second-order effects such as torsional moments, in-plane forces, and shear, and the ability of the procedures to capture these.

The first set of specimens examined was a series of plates tested by Polak (1994). The specimens were 1625 mm square in plan, and 316 mm thick (see Fig. 4(a)). They were reinforced with orthogonal layers of reinforcement on each face, giving a reinforcement ratio of 1.25% per face in the x-direction, and a reinforcement ratio of 0.42% per face in the y-direction. In the out-of-plane direction (z-direction), a nominal amount of stirrup reinforcement was provided giving a reinforcement ratio of 0.07%. Material strengths and other specimen details are provided by Polak. As illustrated in Fig. 4(b), the specimens differed primarily in the loading conditions imposed. Specimen SM1 was subjected to constant uniaxial bending along the strong axis. The second

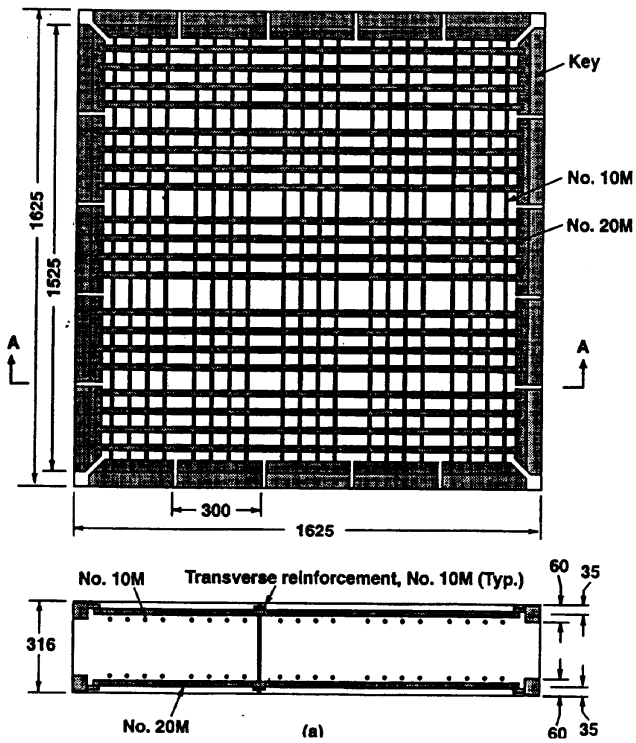

(a) Specimen construction details

Specimen Name	Reinforcement Pattern	Longitudinal Reinforcement ρ_x^*	Longitudinal Reinforcement ρ_y^*	Load Case	Loading Ratio
SM1		1.25%	0.42%		-
SM2		1.25%	0.42%		$M/P = 0.25$ m
SM3		1.25%	0.42%		$M_x/M_y = 3.2$

* per layer

(b)

(b) Loading conditions

Fig. 4 Shell elements tested by Polak (1994)

specimen, SM2, was loaded similarly to the first, but with an axial tension co-acting in the direction of bending, and an axial compression applied in the transverse direction. Specimen SM3 was subjected to biaxial bending. Loads were imposed using a specially devised testing rig (the Shell Element Tester at the University of Toronto).

A one-element mesh was sufficient to model the first specimen because of the uniform moment throughout. The other two were represented by a 3×3 grid of elements. Because of the presence of axial loads, it was necessary to use the Mode 3 approximate analysis procedure. For comparison purposes, the specimens were also analysed using the nonlinear shell analysis program RASP. Shown in Fig. 5 are the predicted and observed moment-curvature responses in the x-direction. It can be seen that behaviour is well represented at all stages of loading for all three specimens. Cracking loads, pre- and post-cracking stiffness, yield loads, ultimate loads, and post-yielding ductility are accurately simulated. There is a slight over-prediction of stiffness at intermediate load levels, indicating that the tension stiffening formulation is perhaps predicting insufficient decay in the post-cracking tensile stresses in the concrete. As well, ignoring the Poisson's effect may have contributed somewhat to the overpredictions of stiffness. Strain-hardening influences, particularly evident in the observed SM2 response, was not modelled and therefore not represented. All three specimens failed by ductile yielding of the reinforcement in the x-direction. In SM3, failure was accompanied by yielding of the reinforcement and crushing of the concrete on the compression face. These failure modes were correctly predicted by the

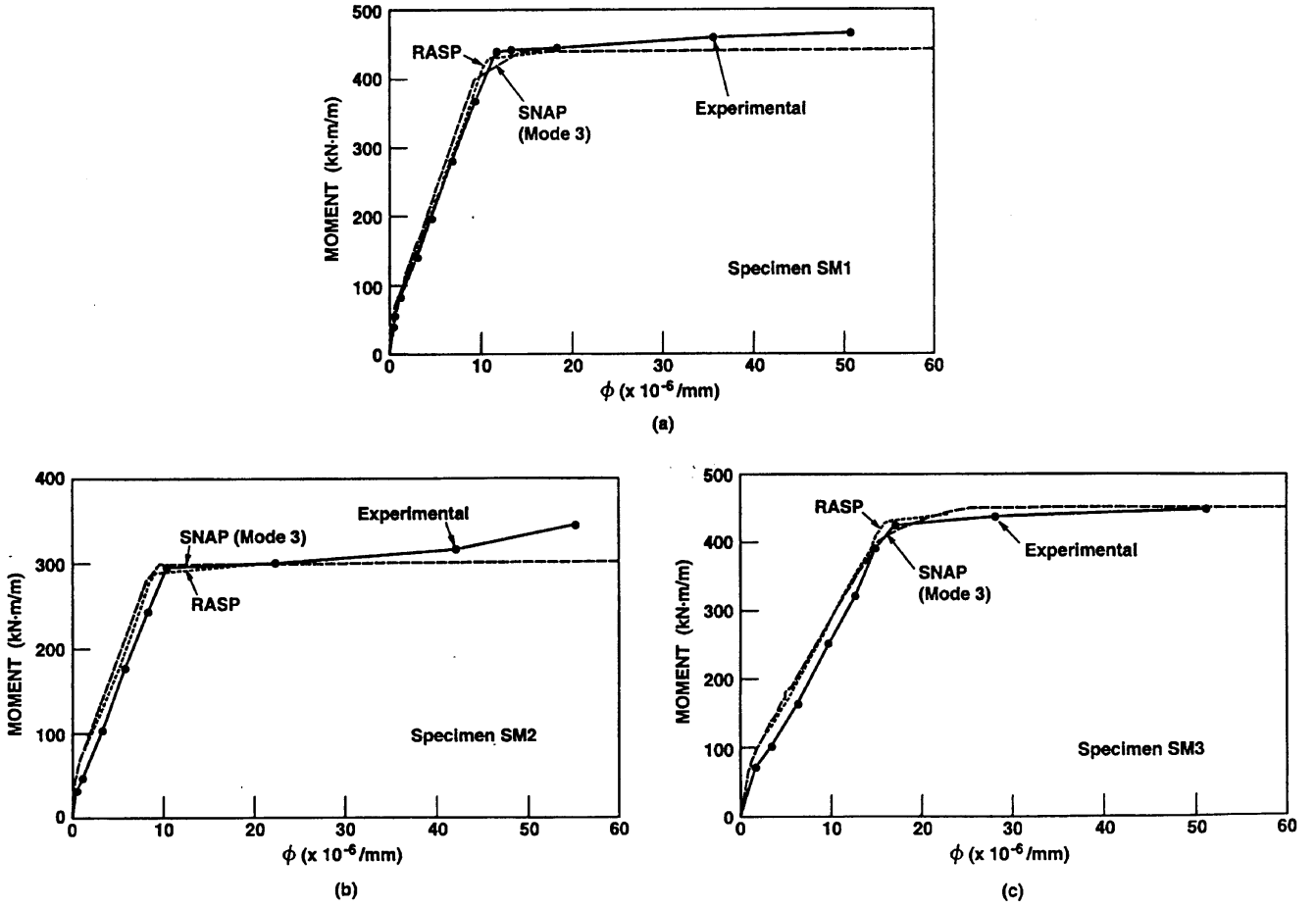

Fig. 5 Comparison of predicted and observed responses for Polak specimens

approximate analyses. As well, the approximate analyses provided similarly accurate predictions of the concrete surface strains, cracking characteristics, and reinforcement strains. Also evident in the response curves is that the approximate solution does not sacrifice much accuracy compared to the full nonlinear shell analysis in this case.

The second set of specimens examined consisted of square corner-supported slabs subjected to a point load applied at the center. This set includes one specimen tested by McNiece (1971) and four tested by Vecchio, Agostino and Angelakos (1993).

The McNiece slab is one often used as a benchmark for calibrating nonlinear analyses. The corner supported two-way slab was 915×915 mm square and 44 mm thick, and reinforced with an orthogonal mesh giving a reinforcement ratio of 0.85%. The purpose of the test was to gauge service load deflections, and thus was not loaded to ultimate. In representing this specimen, a 6×6 mesh of elements was used to model one-quarter of the structure. Shown in Fig. 6 are the results of the analyses using all three approximate procedures (SNAP Modes 1, 2, and 3) and the full nonlinear shell analysis (RASP). The indication is that all procedures give comparable and reasonably accurate predictions of deflection at service load levels.

The slabs tested by Vecchio, Agostino and Angelakos (1993) were 2800×2800×150 mm, and were simply supported at the corners (see Fig. 7(a)). The percentages of reinforcement in the orthogonal directions ranged from light to heavy, as indicated in Fig. 7(b). After first being subjected to various restrained thermal loading conditions, the slabs were point-loaded at the centre and loaded to ultimate. (Note that the slabs were extensively cracked prior to this last loading condition, but had not sustained yielding at any point in the loading regime.) Owing to the concentrated loading and corner support conditions, this series of tests represents a stringent

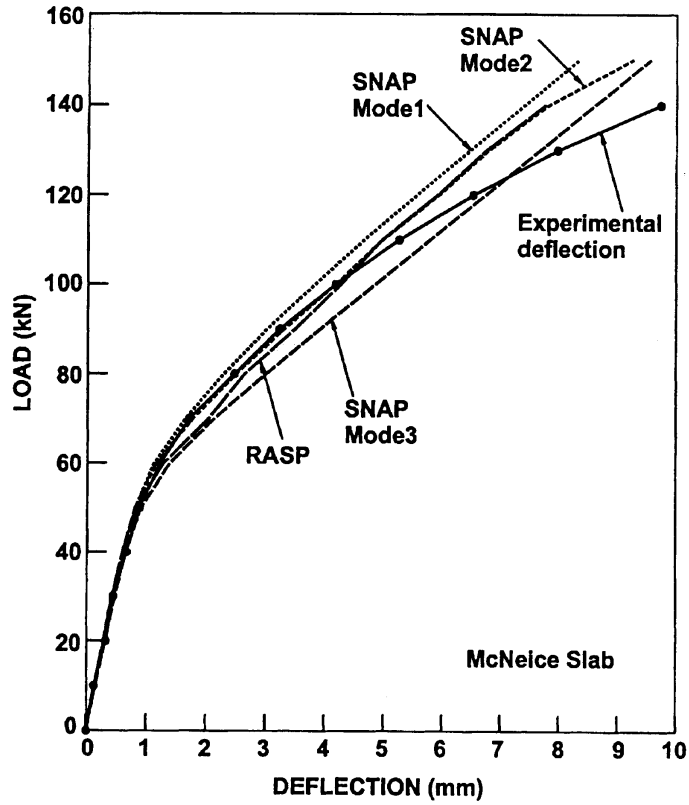

Fig. 6 Comparison of predicted and observed centre deflections of McNiece slab

test of the ability to model two-way action and particularly internal torsional moment effects. The objective here is to gauge the ability of the analysis procedures to accurately represent ultimate capacity.

Taking advantage of symmetry, a quarter-model of the slabs was constructed using a finite element grid of 6×6 elements. Shown in Fig. 8 are the predicted load-displacement responses of the slabs, obtained from the various approximate procedures, together with the experimentally observed response. Also shown is the behaviour obtained from a nonlinear shell analysis (RASP). It is immediately apparent that the correlation is not as favourable as that obtained from the Polak specimens. The disparity in predicted and observed stiffness at low and intermediate load levels is not an issue, since the slabs were extensively cracked due to prior loading. The slabs

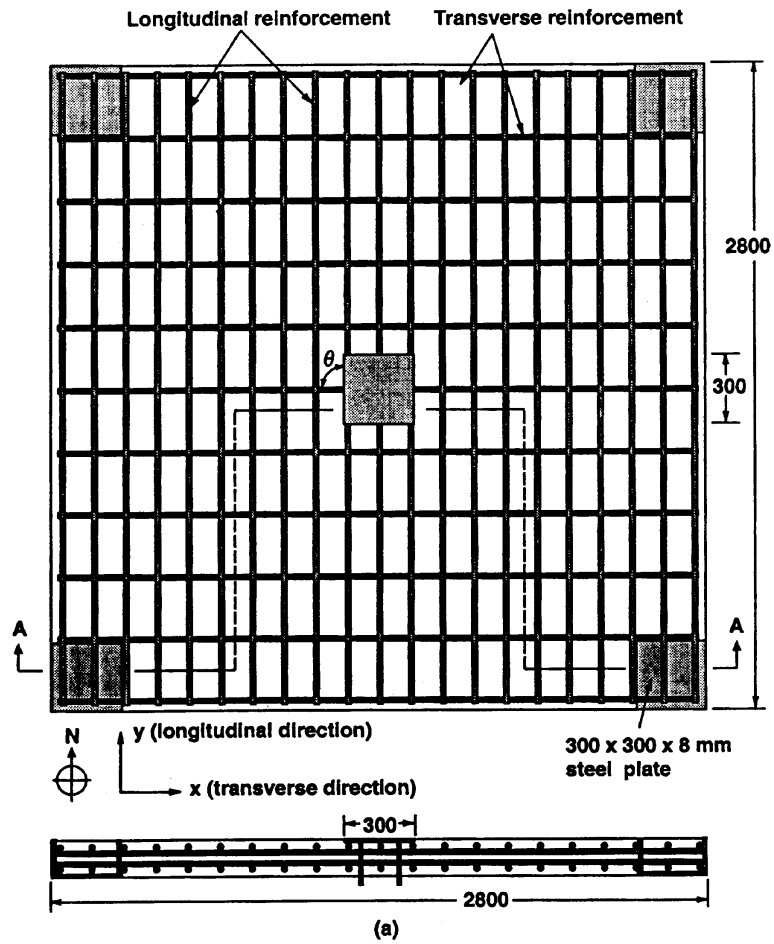

(a)

Specimen	X - Reinforcement			Y - Reinforcement		
	ρ_x* (%)	Bar Type	Spacing (mm)	ρ_y* (%)	Bar Type	Spacing (mm)
TS6	1.50	20M	130	1.50	20M	130
TS7	1.00	20M	200	1.50	20M	130
TS8	0.40	15M	330	1.50	20M	130
TS9	0.40	15M	330	0.75	20M	260

* per layer

(b)

Fig. 7 Details of Agostino/Angelakos plate specimens (Plates were supported at corners, and subjected to point load at centre)

were modelled without consideration of previous load history, and so higher initial stiffnesses were expected. However, what is worrisome is the disparity in the predicted ultimate strengths, particularly with the Mode 2 analyses. For these slabs subjected to high internal torsional moments, the practice of adding the torsional moment M_{xy} to the normal moments (as done in Modes 1 and 3), or the torsional curvature ϕ_{xy} to the normal curvatures (Mode 2), tends to overestimate the resulting decay in strength. Note, however, that the nonlinear shell analysis (RASP) simulates quite well the capacity response of these slabs.

Vecchio and Tang (1990) tested a pair of large-scale column and slab assemblies (see Fig. 9). The slab strips were 100 mm thick and 1500 mm wide. The two intermediately located column stubs were 200 mm in cross section and spaced 3076 mm on centres. A 75 mm drop panel was provided at each column slab joint, and a transverse edge beam was built integral with the slab at each end. The support conditions were a critical aspect of the tests. In both cases, the column bases were fixed against vertical or lateral translation. In the first specimen (TV1), the edge beams were restrained against vertical translation but free to move horizontally. With the second specimen (TV2), the edge beams were restrained against both vertical and lateral translation. The specimens were subjected to a line load applied at the centreline of the middle span. Other pertinent details are provided by Tang. During testing, Specimen TV1 experienced yielding of the bottom longitudinal reinforcement at the midspan, followed by yielding of the top longitudinal reinforcement just beyond the column face. The test then ended somewhat prematurely when a run-away actuator punched through the slab causing a brittle shear failure. The ultimate load of TV1 would thus likely have been higher than that measured and reproduced here. Specimen TV2

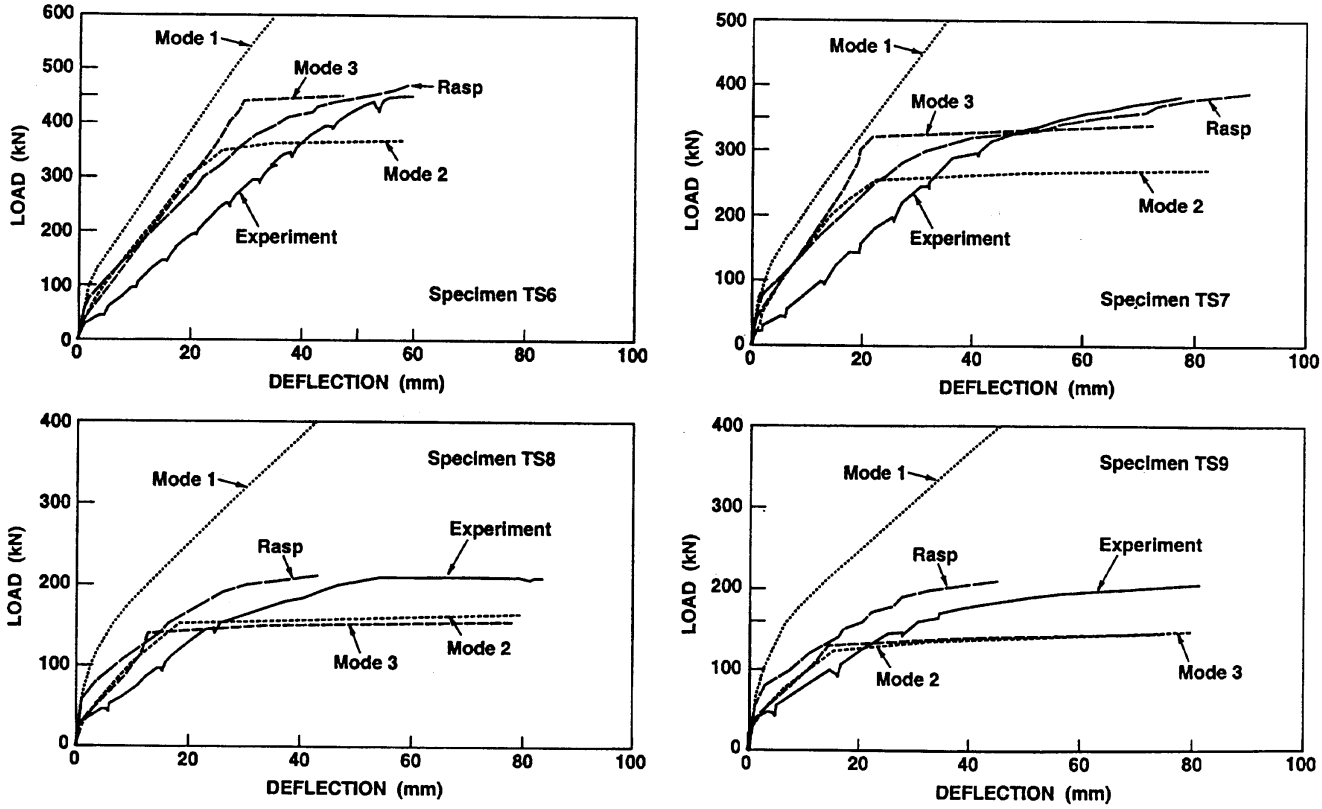

Fig. 8 Comparison of predicted and observed load-deflection responses of Agostino/Angelakos specimens

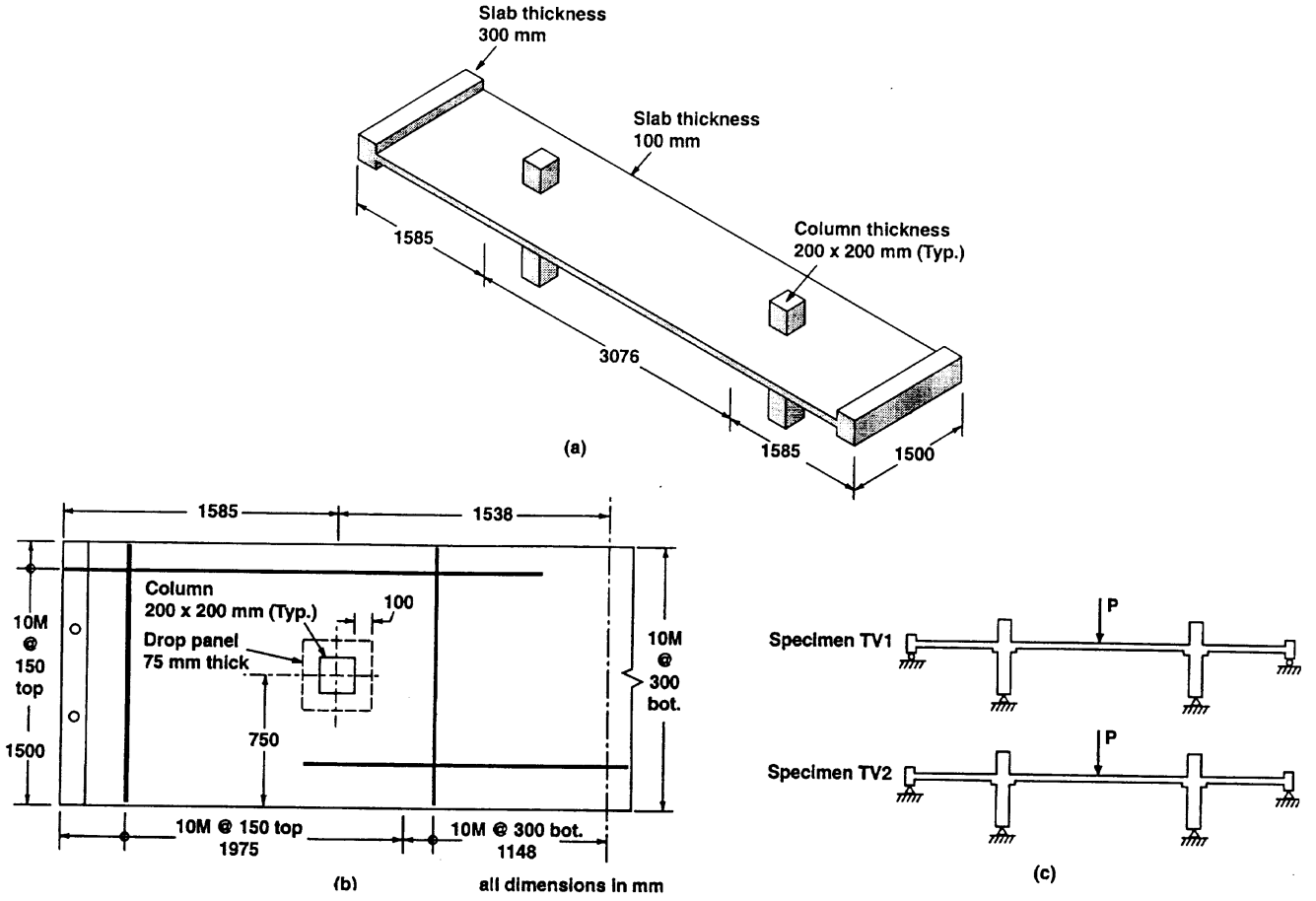

Fig. 9 Details of Tang column strip specimens

benefitted from pronounced compressive membrane action, with the induced axial compression reaching magnitudes of 382 kN (more than four times the applied transverse load!) before experiencing failure. Ultimately, a three-hinge mechanism developed with yielding across the midspan and interior column faces.

A quarter-model of the test specimens was constructed using a relatively course grid of 32 elements (16×2). Both approximate (Mode 3) and full nonlinear analyses were undertaken of the two specimens. Shown in Fig. 10 are the observed and predicted centre-point load-deflection responses. In the case of Specimen TV1, the approximate analysis provided a reasonable representation of the observed behaviour. The strength and stiffness were somewhat overestimated by the approximate analyses. Bear in mind, however, that the observed specimen ultimate capacity was artificially reduced because of the accident experienced during loading, as described above. Also, the slab stiffness was somewhat reduced due to the presence of existing cracks arising from shrinkage and handling. Cracking patterns, concrete surface strains, and reinforcement stresses were modelled with reasonable accuracy. The improvement in the predicted response obtained from the full nonlinear shell analysis (RASP) is marginal. With Specimen TV2, however, the approximate analysis is unsuccessful in accurately modelling behaviour. With the very high levels of axial compression induced by the fixed support conditions, significant overpredictions of strength can arise if axial strains are grossly misjudged, as they can be when geometric nonlinearities are not taken into account. By considering geometric nonlinearities in the RASP analysis, a more accurate representation of strength and stiffness is observed. Note that specimen

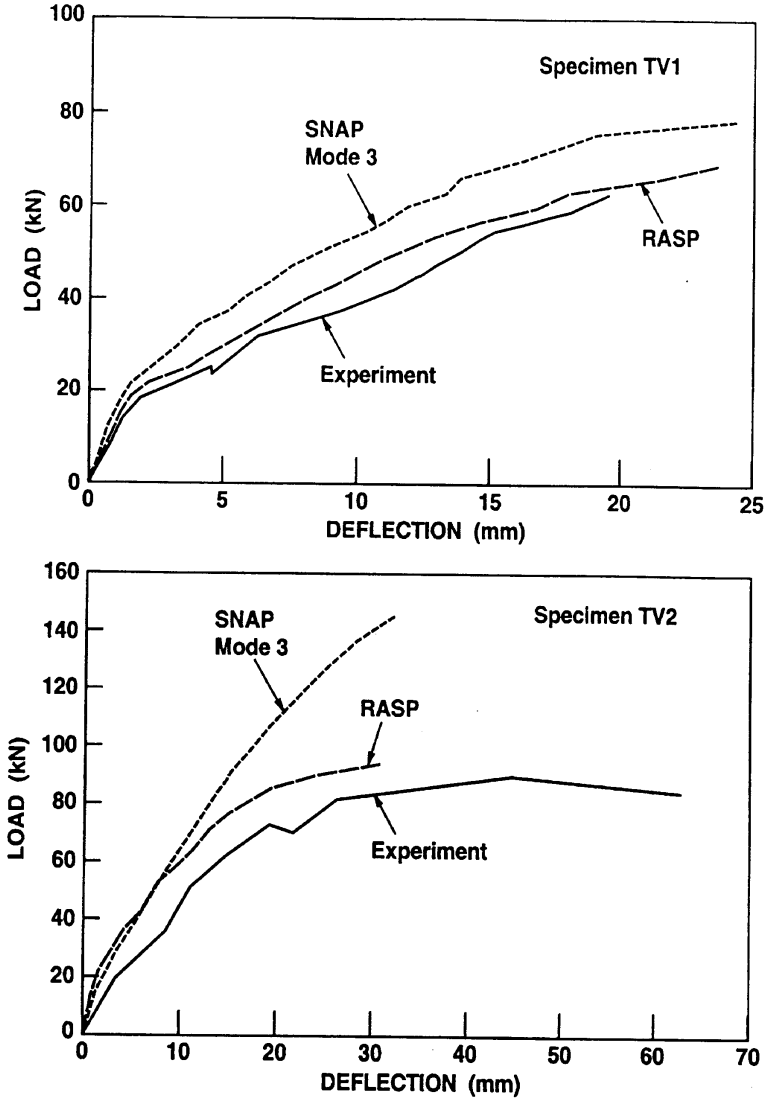

Fig. 10 Comparison of predicted and observed load-deflection responses at the centres of the Tang specimens

TV2 demonstrated a load capacity 32% greater than that of TV1, owing entirely to the influence of the axial compressions induced by the lateral restraints at the supports. Quantifying this second-order influence is a difficult analytical problem, and not one expected to be handled well by an approximate procedure.

9. Conclusions

Reinforced concrete flat plate structures, as a subset of shell structures, typically have structural properties and loading conditions which require much less rigorous second-order analyses than do general three-dimensional shells. By bypassing the geometric nonlinearity algorithms and general three-dimensional stress formulations, which are typically of minor relevance to plates, the analyses can be executed more expediently. Further, various approximate formulations can be implemented which will further reduce the arduous nature of the calculations. This will facilitate

the use of such analysis programs as general design office tools, or as a background engine for automated analysis/design packages.

One alternative approximate procedure is to implement an effective stiffness formulation. This can be done either by incorporating semi-empirical formulations such as Branson's formula, or by adapting a layered sectional analysis algorithm. Alternatively, a plate-bending analysis can be coupled with an in-plane force analysis, and the behaviours described can be enforced by the use of the unbalanced force procedure. Once again, the nonlinear behaviour enforced would be that obtained from an appropriate nonlinear section analysis.

From the calibration tests undertaken, and from corroborations with test data, the following conclusions can be made:

1) For analyses at service load levels, where yielding is not expected at any location in the structure, an effective stiffness formulation based on Branson's formula provides surprisingly good accuracy in terms of load-deflection response. Furthermore, the analyses require little computational effort relative to the other approximate procedures, and much less than a full nonlinear shell analysis. This procedure cannot make allowance for in-plane load effects or shear effects, however.

2) In cases where post-yielding behaviour must be considered, reasonable accuracy can be obtained by using an effective stiffness procedure based on a layered section analysis. The layered section analysis provides the means to rigorously consider nonlinear behaviour by implementing an appropriate set of constitutive laws, and by satisfying sectional equilibrium and compatibility requirements. Once again, however, shear or in-plane load effects cannot be readily considered.

3) Where in-plane load effects (including prestressing) or out-of-plane shear effects are judged to be of some significance, a viable approximate analysis can be obtained by coupling a plate bending analysis and an in-plane force analysis. Nonlinear sectional behaviour is then enforced with the addition of unbalanced forces to the force matrix.

4) When axial force effects are a major influencing factor, such as in cases where support restraints induce high levels of axial compression and arch action, then a full nonlinear shell analysis is required to properly model behaviour. It may also be required when the plate includes nonstandard details such as skewed reinforcement.

5) When the support and loading conditions are such as to produce high internal torsional moments, the approximate procedures show significant deterioration in accuracy when determining ultimate capacity. Again, in these situations, it is advisable to use a full nonlinear shell analysis.

6) If an approximate analysis can be undertaken within the constraints identified above, the analysis will generally be much more efficient and with little loss in accuracy relative to that from a full nonlinear shell analysis. However, given the rather stringent conditions constraining their applications, the approximate procedures are of limited practical value. Future work will be directed towards improving the efficiency of the nonlinear shell analysis procedures.

References

Branson, D.E. (1963). "Design procedures for computing deflections", *J. ACI*, **65**(9), 730.

Cook, R.D., Malkus, D.S. and Plesha, M.E. (1989). *Concepts and Applications of Finite Element Analysis*, 3rd Ed., John Wiley & Sons.

Hinton, E. and Owen, D.R.J. (1984). *Finite Element Software for Plates and Shells*, Pineridge Press

Ltd., Swansea, U.K.
Hu, H. and Schnobrich, W.C. (1990). "Nonlinear analysis of cracked reinforced concrete", *ACI Struct. J.*, **87**(2), 199-207.
Jofriet, J.C. and McNiece, M. (1971). "Finite element analysis of reinforced concrete slabs", *J. Structural Div., ASCE*, **97**(ST-3), 785-806.
Polak, M.A. and Vecchio, F.J. (1993). "Nonlinear analysis of reinforced concrete shells", *J. Struct. Engrg., ASCE*, **119**(12), 3439-3462.
Polak, M.A. and Vecchio, F.J. (1994). "Reinforced concrete shells elements subjected to bending and membrane loads", *ACI Struct. J.*, **91**(2), 261-268.
Scanlon, A. (1971). "Time dependent deflections of reinforced concrete slabs", *Struct. Engrg. Report No. 38*, Dept. of Civil Engrg., Univ. of Alberta.
Scordelis, A.C. and Chan, E.C. (1987). "Nonlinear analysis of reinforced concrete shells", *Computer Applications in Concrete Technology, ACI SP-98*, Amer. Concr. Inst., 25-57.
Seracino, R. (1995). "Towards improving nonlinear analysis of reinforced concrete shells", M.A.Sc. Thesis, Dept. of Civil Engrg., Univ. of Toronto.
Tata, M. (1996). "Simplified nonlinear finite element analysis of reinforced concrete plates", M.A.Sc. Thesis, Dept. of Civil Engrg., Univ. of Toronto.
Vecchio, F.J. (1997). "Towards cyclic load modelling of reinforced concrete", *ACI Struct. J.*, (in press).
Vecchio, F.J., Agostino, N. and Angelakos, B. (1993). "Reinforced concrete slabs subjects to thermal loads", *CJCE*, **20**(5), 741-753.
Vecchio, F.J. and Collins, M.P. (1986). "The modified compression field theory for reinforced concrete elements subjected to shear", *J. ACI*, **83**(2), 219-231.
Vecchio, F.J. and Collins, M.P. (1988). "Predicting the response of reinforced concrete beams subjected to shear using modified compression field theory", *ACI Struct. J.*, **85**(3), 258-268.
Vecchio, F.J. and Collins, M.P. (1993). "Compression response of cracked reinforced concrete", *J. Struct. Engrg., ASCE*, **119**(12), 3590-3610.
Vecchio, F.J. and Emara, B.E. (1992). "Shear deformations in reinforced concrete frames", *ACI Struct. J.*, **89**(1), 46-56.
Vecchio, F.J. and Tang, K. (1990). "Membrane action in reinforced concrete slabs", *CJCE*, **17**(5), 686-697.